

Journal of
***Mechanics of
Materials and Structures***

**NONLOCAL CONTINUUM MODELS FOR CARBON
NANOTUBES SUBJECTED TO STATIC LOADING**

Quan Wang and Yasuhide Shindo

Volume 1, N° 4

April 2006

 mathematical sciences publishers

NONLOCAL CONTINUUM MODELS FOR CARBON NANOTUBES SUBJECTED TO STATIC LOADING

QUAN WANG AND YASUhide SHINDO

Static and buckling analyses of carbon nanotubes (CNTs) are carried out with newly developed nonlocal continuum models. Small-scale effects are explicitly derived for bending deformation solutions for CNTs subjected to general flexural loading first. Solutions via nonlocal continuum models are expressed by simple terms related to scale coefficients in addition to remaining terms via local continuum models in which the simplicity of the nonlocal continuum models is clearly observed. Discussions on various derivations of Young's modulus for CNTs from existing experimental work in the literature are provided, revealing the applicability of the nonlocal continuum models. In addition, a simple equation for the buckling load of CNTs with various general boundary conditions subject to axial loading via the nonlocal elastic beam model is explicitly derived for instability analysis. The results of this research provide benchmark solutions for the response of CNTs subject to general static loading, with small-scale effects modeled and revealed. Thus, the work has great potential in studying mechanical properties of CNTs of various sizes.

1. Introduction

Carbon nanotubes (CNTs) have been the focus of extensive research [Ball 2001; Baughman et al. 2002; Harris 1999; Treacy et al. 1996] since they were discovered by Iijima [1991], because of their potential to lead to new applications, such as frictionless nanoactuators, nanomotors, nanobearings, and nanosprings [Lau 2003].

Two major analytical approaches are used in studies of CNTs. The first is atomic modeling, and includes techniques such as classical molecular dynamics (MD) [Iijima et al. 1996; Yakobson et al. 1997], tight binding molecular dynamics (TBMD) [Hernandez et al. 1998] and density functional theory (DFT) [Sanchez-Portal et al. 1999]. Its use is limited to the study of systems having a relatively small number of atoms.

The second approach, continuum modeling, is more practical in analyzing carbon nanotubes of large-scale systems. Continuum modeling includes elastic beam

Keywords: Nonlocal continuum models, carbon nanotubes, single-walled carbon nanotubes, elastic beam model, stability analysis.

The authors thank the reviewers for their constructive comments.

and shell models, which have been applied in analyzing static response, stability and vibration of CNTs. Yakobson et al. [1996] studied unique features of fullerenes and developed a continuum shell model to study instability patterns of a CNT under different compressive loads. Ru [2000a; 2000b] proposed the buckling analysis of CNTs with shell models. Parnes and Chiskis [2002] investigated elastic buckling of nanofiber reinforced composites with elastic beam theory. Wang and coworkers [Wang and Varadan 2005; Wang 2005; Wang et al. 2005b] have investigated global and local instability or kinks of CNTs with elastic beam models. In these continuum models, stress at a reference point is defined and considered traditionally to be a functional of the strain field at the exact point in the body; hence the models are usually called *classical* or *local* continuum models. A pioneering work [Zhang et al. 2002] established a nanoscale continuum theory to incorporate interatomic potentials into a continuum analysis in studying the linear modulus of a single-wall CNT. The Young's modulus predicted by that work agreed well with prior experimental results and atomic studies. The simplicity of these continuum models has inspired a great deal of work on CNT mechanical behavior, and this research has shown that continuum mechanics is easy to handle and accurate in predicting much this behavior.

Local continuum models do not admit intrinsic size dependence in elastic solutions of inclusions and inhomogeneities. At nanolength scales, however, size effects often become prominent, and in view of the increasing interest in nanotechnology, they need to be addressed [Sharma et al. 2003]. Wang et al. [2005a] used the Tersoff–Brenner potential and *ab initio* calculations to find the size dependence of CNTs in a thin-shell model. Sun and Zhang [2003] pointed out the limitations of the applicability of classical continuum models in nanotechnology. They indicated the importance of semicontinuum models in analyzing nanomaterials with plate-like geometry. Their results contrast with those obtained from classical continuum models; the values of material properties were found to depend heavily on the thickness of the plate structure. The modeling of such a size-dependent phenomenon has become an active researcher subject [Sheehan and Lieber 1996; Yakobson and Smalley 1997]. One concludes from these works that the applicability of the classical continuum models at small scales may be questionable. At such scales the microstructure of the material, such as the lattice spacing between individual atoms, becomes increasingly important and the discrete structure of the material can no longer be homogenized into a continuum. Therefore, more appropriate continuum models rather than classical or local elastic beam and shell theories are needed in studying the small-scale effect in nanomaterials.

Nonlocal elasticity was first proposed by Eringen [1976; 1983] to account for the scale effect in elasticity, by assuming the stress at a reference point to be a functional of the strain field at *every point* in the body. In this way, the internal size scale

could be considered in the constitutive equations simply as a material parameter. Recently, Pugno and Ruoff [2004] modified continuum fracture mechanics and proposed their fracture quantized mechanics to predict fractures of tiny systems with a given geometry and type of loading occurred at quantized stress.

The application of nonlocal elasticity models to nanomaterials has received attention from the nanotechnology community only recently. Peddieson et al. [2003] proposed a version of nonlocal elasticity for the formulation of an Euler–Bernoulli beam theory. They concluded that nonlocal continuum mechanics could potentially play a useful role in the analysis of phenomena related to nanotechnology applications. Sudak [2003] studied infinitesimal column buckling of CNTs, incorporating van der Waals forces and small-scale effects, and showed that the critical axial strain decreases, compared to the results with classical continuum beam model, where the small length scale increases in magnitude. Zhang et al. [2004] proposed a nonlocal multishell model for the axial buckling of CNTs under axial compression. Their results showed that the effect of the small-scale on axial buckling strain is related to the buckling mode and the length of tubes. Wang [2005] studied the dispersion relations for CNTs considering small-scale effects. A qualitative validation study showed that results based on the nonlocal continuum mechanics are in agreement with the published experimental reports in this field.

These studies of the use of nonlocal continuum mechanics in the mechanical analysis of CNTs have shown that nonlocal continuum mechanics is not significantly harder to apply than local continuum mechanics. In existing buckling and vibration analyses of CNTs, the results can all be expressed concisely; only a few terms related to scale coefficients need be included in addition to those based on local continuum models. The simplicity of nonlocal continuum mechanics implies that these proposed nonlocal elastic models, such as nonlocal elastic beam and shell models, have great potential in the study of scale effects, in cases where such effects have to be taken into account (which cannot be done via local continuum mechanics).

In this article we focus on the static and buckling analysis of CNTs using nonlocal continuum models. We first derive explicitly the small-scale effect in the bending analysis of single-walled CNTs subjected to general loading; one clearly observes a difference in response between the local and nonlocal continuum models for this problem. To our knowledge, no experimental data based on CNT static measurements are available yet that would reflect scale effects. Wang [2005] studied the validity and applicability of nonlocal continuum models using experimental data for *vibrating* CNTs only.

To qualitatively show the scope of the proposed research, we show how to derive the Young's modulus of a CNT from experiments, using the force-displacement relation, in such a way that small-scale effects, in particular systems studied in

the literature, can be identified and estimated from published measurements of the Young's modulus.

We next derive solutions for the buckling load of a CNT subjected to axial loading with various boundary conditions, using the nonlocal continuum model, relating these solutions to those obtained with local continuum models. In all simulations, the results of static and buckling analyses are expressed in simple terms related to scale coefficients, in addition to the terms corresponding to local continuum models. This shows the simplicity of the nonlocal continuum models. It is hoped that this work will help provide benchmark solutions for the analysis of CNTs via continuum models.

2. Elastic nonlocal beam models for CNT analysis

According to the theory of nonlocal elasticity [Eringen 1976], the stress at a reference point x is considered to be a functional of the strain field at every point in the body. This observation is in accordance with the atomic theory of lattice dynamics and experimental observations on phonon dispersion. In the limit when the effects of strains at points other than x is neglected, one obtains the classical (local) theory of elasticity. The basic equations for linear, homogeneous, isotropic, nonlocal elastic solid with zero body force are given by

$$\begin{aligned}\sigma_{ij,j} &= 0, \\ \sigma_{ij}(x) &= \int \alpha(|x-x'|, \tau) C_{ijkl} \varepsilon_{kl}(x') dV(x') \text{ for } x \in V, \\ \varepsilon_{ij} &= \frac{1}{2}(u_{i,j} + u_{j,i}),\end{aligned}$$

where C_{ijkl} is the elastic module tensor of classical isotropic elasticity, σ_{ij} and ε_{ij} are the stress and strain tensors, and u_i is displacement vector.

Next,

$$\alpha(|x-x'|, \tau)$$

is the *nonlocal modulus* or attenuation function, which serves to incorporate into the constitutive equations the nonlocal effects at the reference point x produced by local strain at the source x' . Here $|x-x'|$ is the Euclidean distance and τ is the quotient $e_0 a/l$ [Peddieson et al. 2003], where l is the external characteristic length (crack length, wavelength, etc.), a is an internal characteristic length, which we choose as 0.142 nm, the length of a C-C bond, as in [Sudak 2003]; and e_0 is an adjustable parameter, given as 0.39 in [Eringen 1983], although Sudak [2003] proposed a value in the order of hundreds. Our work suggests that Eringen's value is close to the mark, but it needs to be further verified through experiments or through matching dispersion curves of plane waves with those of atomic lattice dynamics for CNTs.

Wang [2005] made a rough estimate of the scale coefficient e_0a from the available highest frequency of a single-walled CNT in the literature, based on vibration analysis using the nonlocal elastic Timoshenko beam model. The asymptotic frequency was derived there as $\bar{\omega} = 21456/(e_0a)$ if the mass density is $\rho = 2.3 \text{ g/cm}^3$ and the thickness of the nanotube is $t = 0.34 \text{ nm}$. Hence, a conservative evaluation of the scale coefficient is given by the equation above as $e_0a < 2.1 \text{ nm}$ for a single-walled CNT, if the measured frequency value is greater than 10 THz. This value, like the frequency, is radius-dependent.

Eringen [1983] reduced the integral-partial differential equations for this linear nonlocal elasticity problem to singular partial differential equations of a special class of physically admissible kernel. In addition, Hooke’s law for a uniaxial stress state can be determined by

$$\sigma(x) - (e_0a)^2 \frac{d^2\sigma(x)}{dx^2} = E\varepsilon(x), \tag{1}$$

where E is the Young’s modulus of the material.

We now apply Euler–Bernoulli beam theory based on the nonlocal continuum elasticity. The free body diagram of an infinitesimal element of a beam structure subjected to both an axial compression force F and a flexural distributed force $q(x)$ is shown in Figure 1. The equilibrium equation for the vertical force component is easily seen to be

$$\frac{dV}{dx} + q(x) = 0,$$

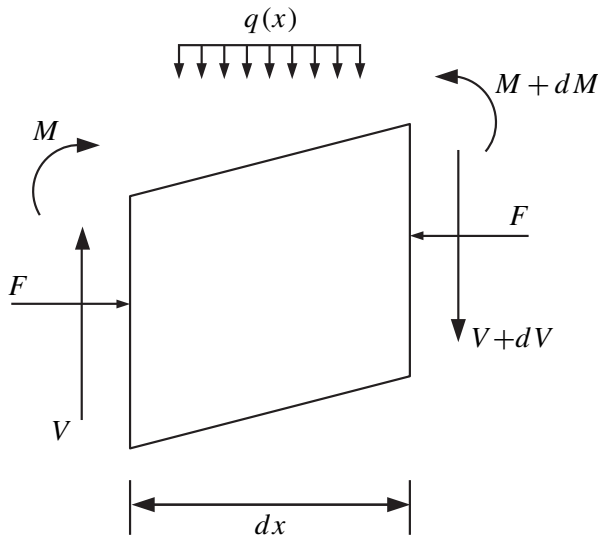


Figure 1. Free body diagram of a beam element.

and that for the moment on the one-dimensional structure is

$$V - \frac{dM}{dx} + F \frac{dw(x)}{dx} = 0, \quad (2)$$

where $V(x, t)$ and $M(x, t)$ are the resultant shear force and bending moment on the beam, and $w(x)$ is the flexural deflection of the beam.

Differentiating the latter equation and substituting into the former one gets

$$\frac{d^2M}{dx^2} = F \frac{d^2w(x)}{dx^2} - q(x). \quad (3)$$

Consider the definitions of the resultant bending moment and the kinematics relation in a beam structure:

$$M = \int_A y \sigma dA \quad \text{and} \quad \varepsilon = -y \frac{d^2w}{dx^2},$$

where y is the coordinate measured from the mid-plane in the height direction of the beam.

Substituting this into the nonlocal constitutive relation Equation (1) leads to

$$M - (e_0a)^2 \frac{d^2M}{dx^2} = -EI \frac{d^2w}{dx^2},$$

where EI is the bending rigidity of the beam structure. Further considering Equation (3) and Equation (2), the expressions for moment and shear force are derived as

$$\begin{aligned} M(x) &= - (EI - F(e_0a)^2) \frac{d^2w(x)}{dx^2} - q(e_0a)^2, \\ V(x) &= -EI \frac{d^3w(x)}{dx^3} - F \frac{d}{dx} \left(w(x) - (e_0a)^2 \frac{d^2w(x)}{dx^2} \right) - (e_0a)^2 \frac{dq(x)}{dx}. \end{aligned} \quad (4)$$

Substitution of the second of these equations into (2) yields the nonlocal elastic beam model for CNTs subjected to static flexural and axial loadings:

$$EI \frac{d^4w(x)}{dx^4} + F \frac{d^2}{dx^2} \left(w(x) - (e_0a)^2 \frac{d^2w(x)}{dx^2} \right) - q(x) \left(1 - (e_0a)^2 \frac{d^2q(x)}{dx^2} \right) = 0. \quad (5)$$

It is easily seen from the derivation that the local Euler–Bernoulli beam model is recovered when the parameter e_0 is identically zero.

3. Flexural bending analysis of CNTs

To investigate the bending analysis of CNTs subjected to static flexural loading, the governing equation for CNTs can be derived from (5) as

$$EI \frac{d^4 w(x)}{dx^4} = q(x) - (e_0 a)^2 \frac{d^2 q(x)}{dx^2}.$$

Hence the model for a CNT subject to a distributed force $q(x)$, concentrated forces P_i at $x = a_i$ ($i = 1 \dots m$), and bending moment M_j at $x = b_j$ ($j = 1 \dots n$) has the form

$$EI \frac{d^4 w(x)}{dx^4} = q(x) - (e_0 a)^2 \frac{d^2 q(x)}{dx^2} + \sum_{i=1}^m P_i (\delta(x - a_i) - (e_0 a)^2 \delta''(x - a_i)) - \sum_{j=1}^n M_j (\delta'(x - b_j) - (e_0 a)^2 \delta'''(x - b_j)), \quad (6)$$

where δ is the Dirac delta function, and $'$ denotes differentiation with respect to x .

By integrating both sides of (6), one obtains expressions for the beam deformation and its three derivatives as follows:

$$w'''(x) = \frac{1}{EI} \int_0^x q(x_1) dx_1 - (e_0 a)^2 \frac{dq(x)}{dx} + C_1 + \sum_{i=1}^m P_i (H(x - a_i) - (e_0 a)^2 \delta'(x - a_i)) - \sum_{j=1}^n M_j (\delta(x - b_j) - (e_0 a)^2 \delta''(x - b_j)), \quad (7)$$

$$w''(x) = \frac{1}{EI} \int_0^x (x - x_1) q(x_1) dx_1 - (e_0 a)^2 q(x) + C_1 x + C_2 + \sum_{i=1}^m P_i ((x - a_i) H(x - a_i) - (e_0 a)^2 \delta(x - a_i)) - \sum_{j=1}^n M_j (H(x - b_j) - (e_0 a)^2 \delta'(x - b_j)), \quad (8)$$

$$w'(x) = \frac{1}{EI} \frac{1}{2} \int_0^x (x - x_1)^2 q(x_1) dx_1 - (e_0 a)^2 \int_0^x q(x_1) dx_1 + \frac{C_1}{2} x^2 + C_2 x + C_3 + \sum_{i=1}^m P_i ((x - a_i)^2 H(x - a_i) / 2 - (e_0 a)^2 H(x - a_i)) - \sum_{j=1}^n M_j ((x - b_j) H(x - b_j) - (e_0 a)^2 \delta(x - b_j)), \quad (9)$$

$$\begin{aligned}
 w(x) = & \frac{1}{EI} \frac{1}{6} \int_0^x (x-x_1)^3 q(x_1) dx_1 - (e_0a)^2 \int_0^x (x-x_1) q(x_1) dx_1 \\
 & + \frac{C_1}{6} x^3 + \frac{C_2}{2} x^2 + C_3 x + C_4 \\
 & + \sum_{i=1}^m P_i ((x-a_i)^3 H(x-a_i)/6 - (e_0a)^2 (x-a_i) H(x-a_i)) \\
 & - \sum_{j=1}^n M_j ((x-b_j)^2 H(x-b_j)/2 - (e_0a)^2 H(x-b_j)). \quad (10)
 \end{aligned}$$

3.1. Cantilevered CNT. Next we discuss small-scale effects on the response of a CNT under different boundary conditions.

We first study a cantilevered CNT of length L subjected to a concentrated force P at $x = l$. This system has been used by Wong et al. [1997] to measure the Young’s modulus. According to (10), the response of the CNT under a point force P is

$$w(x) = \frac{1}{EI} \left(\frac{1}{6} C_1 x^3 + \frac{1}{2} C_2 x^2 + C_3 x + C_4 + \frac{1}{6} P (x-l)^3 H(x-l) - P (x-l) H(x-l) \right).$$

The boundary conditions at the left end, $w(0) = w'(0) = 0$, lead to the solutions having $C_3 = C_4 = 0$. The boundary conditions at the right end, $M(L) = V(L) = 0$, together with Equations (4), lead to

$$\begin{aligned}
 -EI \left. \frac{d^2 w(x)}{dx^2} \right|_{x=L} - P \delta(L-l) (e_0a)^2 = 0, \quad \text{that is,} \quad \left. \frac{d^2 w(x)}{dx^2} \right|_{x=L} = 0, \\
 -EI \left. \frac{d^3 w(x)}{dx^3} \right|_{x=L} - (e_0a)^2 P \delta'(L-l) = 0, \quad \text{that is,} \quad \left. \frac{d^3 w(x)}{dx^3} \right|_{x=L} = 0.
 \end{aligned} \quad (11)$$

Hence C_1 and C_2 can be derived by substituting (7) and (8) into (11):

$$C_1 = -P \quad \text{and} \quad C_2 = Pl.$$

The response of the CNT is therefore

$$w(x) = \frac{1}{EI} \left(\frac{P(x-l)^3}{6} H(x-l) - P (e_0a)^2 (x-l) H(x-l) - \frac{Px^3}{6} + \frac{Plx^2}{2} \right).$$

From this we find that the small-scale term, $P(e_0a)^2(x-l)H(x-l)$, will affect the response of the CNT only in the domain $x > a$. The response at $x = l$ is

$$w(l) = \frac{Pl^3}{3EI}. \quad (12)$$

It is important to determine whether the small-scale term has any effect on the derived Young’s modulus in experimental investigations. In the investigations of

mechanical properties of CNTs by Wong et al. [1997] and Poncharal et al. [1999], the response of a cantilevered CNT at the position of the concentrated force was employed to evaluate Young's modulus of CNTs. According to Equation (12), it is clear that the derived Young's modulus can be viewed as an "accurate" evaluation, since the measurement is independent of the small-scale effect.

Wong et al. [1997] also considered the beam subjected to surface friction force in their modeling of the cantilevered CNT. The friction force can be modeled as a uniform distributed force f applied on the beam. From Equation (10), the response of the CNT can be written as

$$w(x) = \frac{1}{EI} \left(\frac{fx^4}{24} - \frac{fx^2}{2} (e_0a)^2 + C_1x^3/6 + C_2x^2/2 + C_3x + C_4 \right).$$

The fixed left end again leads to $C_3 = C_4 = 0$. Zero moment and shear force at the right end lead to $C_1 = -fL$ and $C_2 = fL^2/2$, by (4), leading to the solution

$$EIw''(L) + (e_0a)^2 f = 0 \quad \text{and} \quad EIw'''(L) = 0.$$

Therefore, the response of the CNT under uniform distributed force is

$$w(x) = \frac{1}{EI} \left(\frac{fx^4}{24} - \frac{fLx^3}{6} + \frac{fL^2x^2}{4} - \frac{fx^2}{2} (e_0a)^2 \right).$$

It can be seen that the small-scale term has an effect on the measurement of mechanical properties for a cantilevered CNT subjected to uniformly distributed force. This effect has to be considered if an independent value for the Young's modulus or any other material properties is to be evaluated properly. The small-scale effect on the deformation of the CNT is studied numerically in terms of the location of the deformation and the length of the CNT by studying the ratio of the response for the nonlocal versus the local continuum models, at $x = l$. In the simulations we take $e_0a = 2$ nm, as suggested in [Wang 2005]. In the top half of Figure 2 we see a plot of this ratio versus the nondimensional location (l/L), for a CNT having length $L = 10$ nm. We see that the small-scale effect is more obvious for the response at the point near the free end. The small-scale effect decreases the response, indicating that its neglect may lead to an overestimation of the Young's modulus from the measurements. In [Wong et al. 1997], an increasing variation of the Young's modulus was found by using the classical beam model when the measurement was towards the free end of the cantilever CNT, with both distributed friction and point loading modeled in their experiment. These authors' findings on the increasing variation of the Young's modulus are in agreement with the result shown in the figure for the nonlocal beam model, in which a decreasing variation of the bending deformation is observed as one moves toward the free end. The effect of the length of the CNT on the ratio is seen in Figure 2, bottom, where

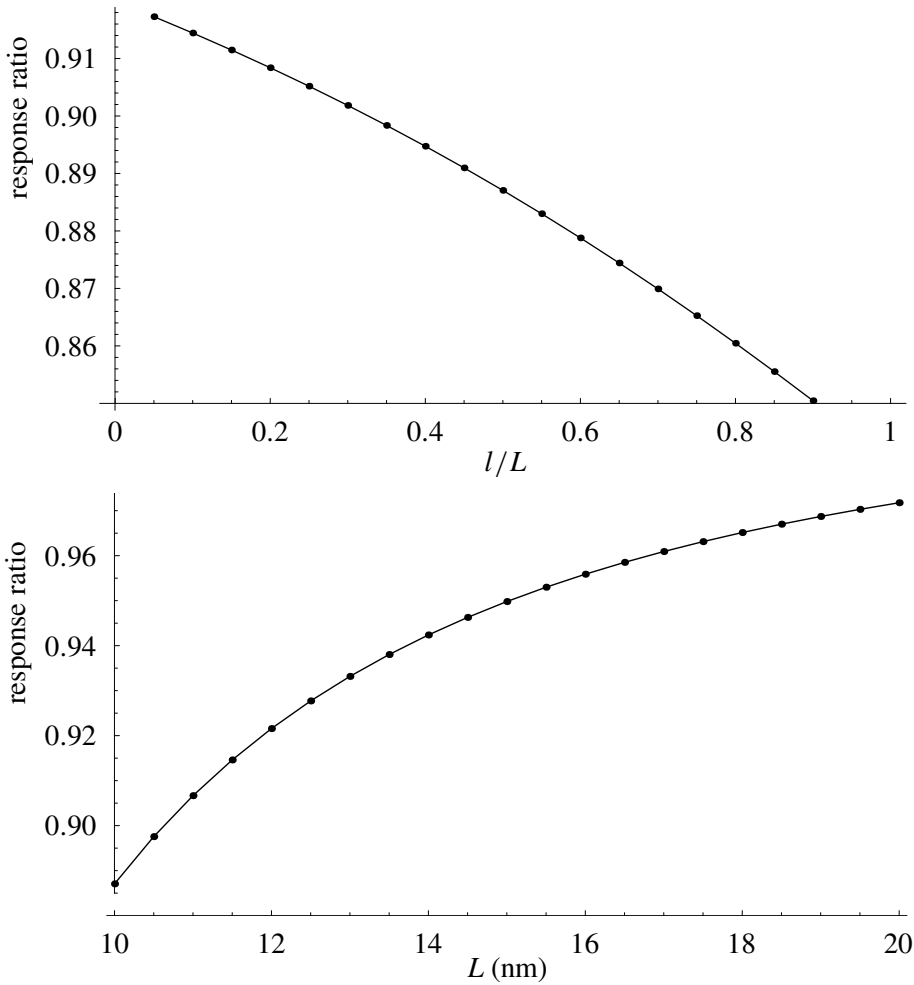


Figure 2. Small-scale effect versus location of the measurement (top) and length of CNT (bottom) for the model of a cantilevered CNT under distributed force.

we take $l/L = 0.5$. It is expected that the small-scale effect is higher for shorter CNTs, and this can be seen in the figure. Thus a local continuum model becomes appropriate for modeling large CNTs.

3.2. Simply supported CNT. Next, the response of a simply supported CNT subjected to a concentrated force P at $x = l$ will be discussed to show the small-scale effect. The governing equation for the CNT can be obtained from (10) as

$$w(x) = \frac{1}{EI} \left(\frac{P(x-l)^3}{6} H(x-l) - P(x-l)H(x-l)(e_0a)^2 + \frac{C_1x^3}{6} + \frac{C_2x^2}{2} + C_3x + C_4 \right). \quad (13)$$

The boundary conditions on the two sides of the CNT, $w(0) = w(L) = M(0) = M(L) = 0$, lead to the solution for the four coefficients, C_1 , C_2 , C_3 and C_4 , and thus the response of the CNT can finally be obtained as:

$$w(x) = \frac{1}{EI} \left(\frac{P(x-l)^3}{6} H(x-l) - P(x-l)H(x-l)(e_0a)^2 - \frac{P(L-l)x^3}{6L} + \frac{P(L-l)(-l^2 + 2Ll)x}{6L} + \frac{P(L-l)(e_0a)^2x}{L} \right).$$

The response of the CNT at the force location, $x = l$, is thus derived as:

$$w(l) = \frac{1}{EI} \left(-\frac{P(L-l)l^3}{6L} + \frac{P(L-l)(-l^2 + 2Ll)l}{6L} + \frac{P(L-l)(e_0a)^2l}{L} \right).$$

Especially when $l = L/2$, one can obtain,

$$w\left(\frac{L}{2}\right) = \frac{L^3}{48EI} \left(1 + 12\left(\frac{e_0a}{L}\right)^2 \right).$$

The study of the small-scale effect on the simply supported CNT is illustrated in Figure 3. The top half of the figure plots the ratio of the response from the local and nonlocal continuum model versus the nondimensional location (l/L) for a CNT with $L = 10$ nm. It is observed that the small-scale effect is more obvious for the response at the two ends of the beam. The effect leads to the value of the ratio up to 2.4. The small-scale effect makes the response of the CNT larger indicating that an under-estimated Young's modulus might be obtained from the measurement of deformation of a simply supported CNT. The effect of the length of the CNT on the ratio is shown in the bottom half of the figure, for $l/L = 0.5$. It is again within our understanding that the small-scale has higher effect for shorter simply supported CNTs.

3.3. Fixed-fixed CNT. Salvetat et al. [1999] investigated the elastic and shear modulus of CNTs by measuring the displacement of a fixed-fixed CNT subjected to a concentrated force. Thus, it is of significance to understand and evaluate the small-scale effect on the results of the moduli by measuring the response of fixed-fixed CNTs. The general expression for the deformation result of a fixed-fixed CNT subjected to a concentrated force P at $x = l$ is same as Equation (13). Considering the boundary conditions at the two ends of the beam, $w(0) = w'(0) = w(L) =$

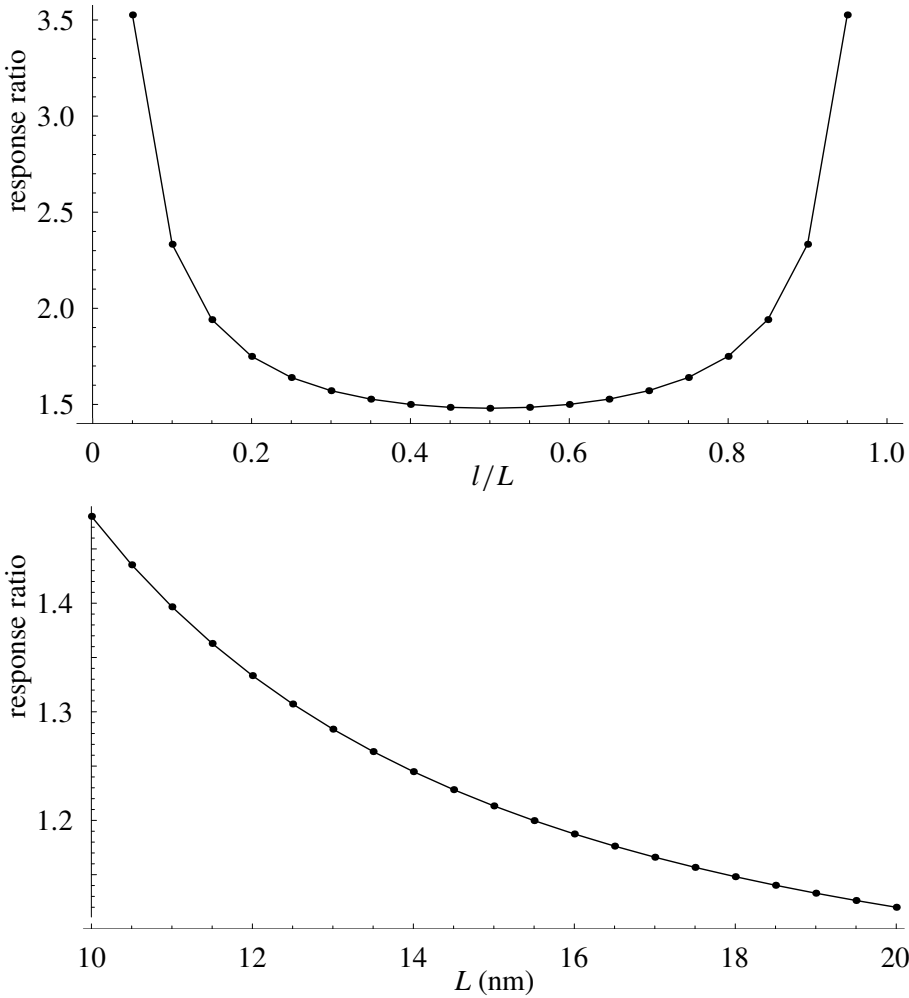


Figure 3. Small-scale effect versus location of the measurement (top) and length of CNT (bottom) for a singly supported CNT.

$w'(L) = 0$, one can obtain the values for the four coefficients, C_1 , C_2 , C_3 and C_4 , and hence, the response of the beam shown as

$$w(x) = \frac{1}{EI} \left(\frac{P(x-l)^3}{6} H(x-l) - P(x-l)H(x-l)(e_0a)^2 + \left(\frac{P(e_0a)^2}{L^2} \left(\frac{2l}{L} - 1 \right) - \frac{P(L-l)^2}{6L^2} \left(1 + \frac{2l}{L} \right) \right) x^3 + \left(\frac{P(e_0a)^2}{L^2} (2L - 3l) + \frac{P(L-l)^2 l}{2L^2} \right) x^2 \right).$$

The expression for the response at $x = l$ is thus given as:

$$w(x) = \frac{1}{EI} \left(\left(\frac{P(e_0a)^2}{L^2} \left(\frac{2l}{L} - 1 \right) - \frac{P(L-l)^2}{6L^2} \left(1 + \frac{2l}{L} \right) \right) x^3 + \left(\frac{P(e_0a)^2}{L^2} (2L - 3l) + \frac{P(L-l)^2 l}{2L^2} \right) x^2 \right).$$

Furthermore, the result for $l = L/2$ is given as:

$$w\left(\frac{L}{2}\right) = \frac{PL^3}{192} \left(1 + 24 \left(\frac{e_0a}{L} \right)^2 \right).$$

Figure 4, top, shows the ratio of the response from the local and nonlocal continuum model versus the nondimensional location (l/L), for $L = 10$ nm. It is seen clearly that the ratio reaches 3.7 when the measurement is taken near fixed ends and 1.96 for measurement at the center of the beam. This observation indicates that the Young’s modulus may be underestimated by a factor of at least two in the fixed-fixed CNT. The bottom half of the figure again shows the effect of the length of the CNT on the estimation of the response, if the measurement point is taken at the middle of the CNT. It is seen that the small-scale effect is still obvious for a CNT with $L = 15$ nm although this effect becomes smaller with longer CNTs.

From the numerical simulation on three types of CNTs, it is found that the small-scale effects are more obvious for stiffer CNTs, i.e. fixed-fixed CNTs, and less obvious for softer CNTs, i.e. cantilevered CNTs. Since the experimental results in [Salvetat et al. 1999] are inconsistent, the verification for the nonlocal beam model cannot be implemented at the moment, but will be conducted when consistent data are available. However, the scale effect was truly observed in [Salvetat et al. 1999].

4. Buckling analysis of CNTs

Buckling is one type of instability exhibited by structures subjected to compressive loading. Sudak [2003] derived the buckling load of simply supported CNTs via the nonlocal continuum model. To establish the relationship between the buckling load of CNTs considering small-effect from nonlocal continuum models and that without taking into account of small-effect from local continuum models is the main objective in this section.

The governing equation for a CNT subjected to a compressive loading, F , is given as follows according to Equation (5):

$$EI \frac{d^4 w(x)}{dx^4} + F \frac{d^2}{dx^2} \left(w(x) - (e_0a)^2 \frac{d^2 w(x)}{dx^2} \right) = 0. \tag{14}$$

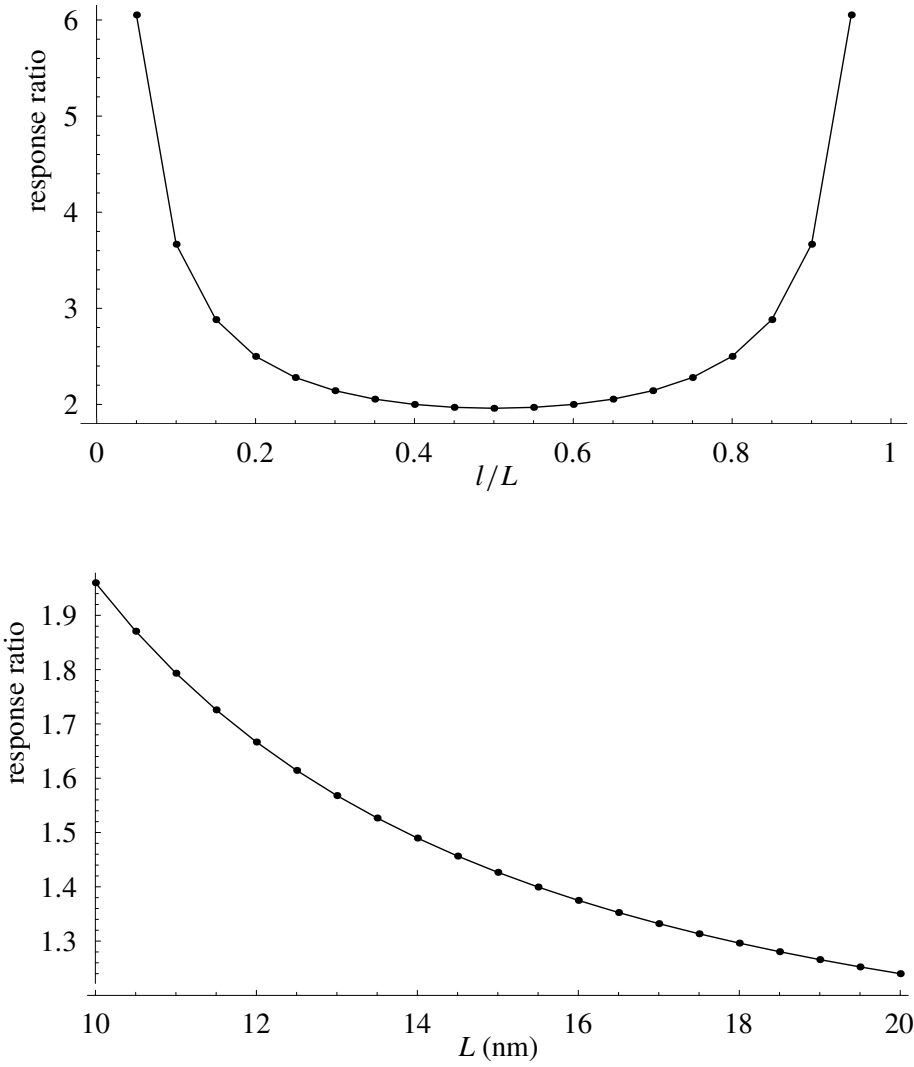


Figure 4. Small-scale effect versus location of the measurement (top) and length of CNT (bottom) for a fixed-fixed CNT.

The general solution for Equation (14) can be easily derived as:

$$w(x) = A_1 \cos \alpha x + A_2 \sin \alpha x + A_3 x + A_4, \tag{15}$$

where $\alpha = \sqrt{\frac{F}{EI - F(e_0 a)^2}}$.

The buckling load can be derived from an eigenvalue problem to find nontrivial solution for $w(x)$ by substituting Equation (15) into four boundary conditions at

the ends of beams. The fundamental value of α for the first buckling mode is derived as follows [Timoshenko and Gere 1963]:

$$\alpha = \frac{\beta\pi}{L}, \quad (16)$$

where β has different value for beams with different boundary conditions, i.e. $\beta = 1$ for simply supported beams; $\beta = 0.5$ for cantilevered beams; $\beta = 2$ for fixed-fixed beams. From Equation (16), the buckling load for CNTs with the nonlocal continuum model can thus be obtained as

$$F = \frac{EI\left(\frac{\beta\pi}{L}\right)^2}{1 + (e_0a)^2\left(\frac{\beta\pi}{L}\right)^2}. \quad (17)$$

It can be seen clearly that the buckling load becomes smaller with a factor

$$\left(1 + (e_0a)^2\left(\frac{\beta\pi}{L}\right)^2\right)^{-1} \quad (18)$$

from the nonlocal elastic beam theory compared to that from local continuum model. Equation (17) provides a general solution for the buckling load with the nonlocal continuum model. For example, the solution for buckling load at $\beta = 1$ for a simply supported CNT was provided by Sudak [2003]. From the solution shown in (17), it can be concluded that the small-scale effect is more obvious for shorter, or smaller L , and stiffer CNT, or higher β . Yakobson et al. [1996] studied the instability behavior of CNTs by using molecular dynamics. In their results on the instability patterns, they found a beam-like buckling mode with two half wavenumber in tube length direction at the axial compression strain $\varepsilon = 0.09$ for a CNT with length 6 nm and diameter 1 nm. However, according to the continuous elastic beam model [Wang and Varadan 2005], the CNT may have its beam-like buckling for a two-half wavenumber mode only at compression strain $\varepsilon = 0.137$. Such discrepancy of the derived buckling strain may be due to the scale effect. From the currently developed nonlocal theory, it can be easily found that the over-estimated buckling strain can be modulated to match the result from the molecular dynamics calculations in [Yakobson et al. 1996] if the scale coefficient is set to be $e_0a = 1.2$ nm. It is also noted that the nonlocal beam model cannot capture the radius-dependent scale effect since in beam model, a uniform radial deformation assumption is endorsed. The possible radius-dependent scale effect found in [Wang et al. 2005a] could only be evaluated from a nonlocal shell model which will be developed and studied later.

5. Conclusions

Small-scale effects on both the bending analysis of CNTs subjected to static flexural loading and the buckling load of CNTs subjected to compressive loading are explicitly studied with the nonlocal continuum beam theory. It is found that there is no such effect on the static response of a cantilevered CNT at the location where the beam is subjected to a concentrated force, and hence the experimental work on the measurement of Young's modulus of CNTs on a cantilevered CNT subjected to concentrated force is relatively reliable since the small-scale effect of CNTs is not involved in the measurement of the response. On the other hand, the small-scale effects are explicitly derived on the response of cantilevered CNT subjected to distributed force at all locations, simply supported CNTs and fixed-fixed CNTs at the location where the CNT is subjected to concentrated force. The effect becomes more obvious with smaller size of CNTs. In addition, the effect is dependent on the location where the response is taken. For example, the effect is higher on the responses, where the force is applied at the two ends of both simply supported and fixed-fixed CNTs. But the effect is higher at the free end of a cantilevered CNT subjected to a uniformly distributed force. The results also reveals that the small-scale effects are more obvious for stiffer CNTs, i.e. fixed-fixed CNTs, and less obvious for softer CNTs, i.e. cantilevered CNTs. The results on buckling instability of CNTs show that the buckling load becomes smaller when small-scale effect is considered by the nonlocal continuum model. The ratio of the result from nonlocal model to that via local model is explicitly derived for CNTs with any general boundary conditions. Furthermore, the small-scale effect is found to be more obvious for shorter and stiffer CNT in buckling analysis. Further studies may focus on the corresponding analysis of multi-walled CNTs. In all simulations, the results for CNTs static and buckling analyses are all expressed by simple terms related to scale coefficients in addition to terms by local continuum models. Thus, the simplicity of the nonlocal continuum mechanics is well seen and the applicability of the theory is promising.

References

- [Ball 2001] P. Ball, "Roll up for the revolution", *Nature* **414**:6860 (2001), 142–144.
- [Baughman et al. 2002] R. H. Baughman, A. A. Zakhidov, and W. A. de Heer, "Carbon nanotubes – the route toward applications", *Science* **297**:5582 (2002), 787–792.
- [Eringen 1976] A. C. Eringen, *Nonlocal polar field models*, Academic Press, New York, 1976.
- [Eringen 1983] A. C. Eringen, "On differential equations of nonlocal elasticity and solutions of screw dislocation and surface waves", *J. Appl. Phys.* **54**:9 (1983), 4703–4710.
- [Harris 1999] P. J. F. Harris, *Carbon nanotubes and related structures*, Cambridge University Press, Cambridge, 1999.

- [Hernandez et al. 1998] E. Hernandez, C. Goze, P. Bernier, and A. Rubio, “Elastic properties of C and $B_xC_yN_z$ composite nanotubes”, *Phys. Rev. Lett.* **80**:20 (1998), 4502–4505.
- [Iijima 1991] S. Iijima, “Helical microtubules of graphitic carbon”, *Nature* **354**:6348 (1991), 56–58.
- [Iijima et al. 1996] S. Iijima, C. Brabec, A. Maiti, and J. Bernholc, “Structural flexibility of carbon nanotubes”, *J. Chem. Phys.* **104**:5 (1996), 2089–2092.
- [Lau 2003] K. T. Lau, “Interfacial bonding characteristics of nanotube/polymer composites”, *Chem. Phys. Lett.* **370**:3–4 (2003), 399–405.
- [Parnes and Chiskis 2002] R. Parnes and A. Chiskis, “Buckling of nano-fibre reinforced composites: a reexamination of elastic buckling”, *J. Mech. Phys. Solids* **50**:4 (2002), 855–879.
- [Peddieson et al. 2003] J. Peddieson, G. R. Buchanan, and R. P. McNitt, “Application of nonlocal continuum models to nanotechnology”, *Int. J. Eng. Sci.* **41**:3–5 (2003), 305–312.
- [Poncharal et al. 1999] P. Poncharal, Z. L. Wang, D. Ugarte, and W. de Heer, “Electrostatic deflections and electromechanical resonances of carbon nanotubes”, *Science* **283**:5407 (1999), 1513–1516.
- [Pugno and Ruoff 2004] N. Pugno and R. Ruoff, “Quantized fracture mechanics”, *Philos. Mag.* **84**:27 (2004), 2829–2845.
- [Ru 2000a] C. Q. Ru, “Effective bending stiffness of carbon nanotubes”, *Phys. Rev.* **B62**:15 (2000), 9973–9976.
- [Ru 2000b] C. Q. Ru, “Elastic buckling of single-walled carbon nanotubes ropes under high pressure”, *Phys. Rev.* **B62**:15 (2000), 10405–10408.
- [Salvetat et al. 1999] J. P. Salvétat, G. A. Briggs, J. M. Bonard, R. R. Bacsá, A. J. Kulik, T. Stockli, N. A. Burnham, and L. Forro, “Elastic and shear moduli of single-walled carbon nanotube ropes”, *Phys. Rev. Lett.* **82**:5 (1999), 944–947.
- [Sanchez-Portal et al. 1999] D. Sanchez-Portal, E. A. and J. M. Soler, A. Rubio, and P. Ordejon, “Ab initio structural, elastic, and vibrational properties of carbon nanotubes”, *Phys. Rev.* **B59**:19 (1999), 12678–12688.
- [Sharma et al. 2003] P. Sharma, S. Ganti, and N. Bhate, “Effect of surfaces on the size-dependent elastic state of nano-inhomogeneities”, *Appl. Phys. Lett.* **82**:4 (2003), 535–537.
- [Sheehan and Lieber 1996] P. E. Sheehan and C. M. Lieber, “Nanotribology and nanofabrication of MoO_3 structures by atomic force microscopy”, *Science* **272**:5265 (1996), 1158–1161.
- [Sudak 2003] L. J. Sudak, “Column buckling of multiwalled carbon nanotubes using nonlocal continuum mechanics”, *J. Appl. Phys.* **94**:11 (2003), 7281–7287.
- [Sun and Zhang 2003] C. T. Sun and H. Zhang, “Size-dependent elastic moduli platelike nanomaterials”, *J. Appl. Phys.* **93**:2 (2003), 1212–1218.
- [Timoshenko and Gere 1963] S. P. Timoshenko and J. M. Gere, *Theory of elastic stability*, McGraw-Hill, New York, 1963.
- [Treacy et al. 1996] M. M. J. Treacy, T. W. Ebbesen, and J. M. Gibson, “Exceptionally high Young’s modulus observed for individual carbon nanotubes”, *Nature* **381**:6584 (1996), 678–680.
- [Wang 2005] Q. Wang, “Wave propagation in carbon nanotubes via nonlocal continuum mechanics”, *J. Appl. Phys.* **98** (2005), 124301.
- [Wang and Varadan 2005] Q. Wang and V. K. Varadan, “Stability analysis of carbon nanotubes via continuum models”, *Smart Mater. Struct.* **14** (2005), 281–286.
- [Wang et al. 2005a] L. Wang, Q. Zheng, J. Liu, and Q. Jiang, “Size dependence of the thin-shell model for carbon nanotubes”, *Phys. Rev. Lett.* **95** (2005), 105501.

- [Wang et al. 2005b] Q. Wang, T. Hu, G. Chen, and Q. Jiang, “Bending instability characteristics of double-walled carbon nanotubes”, *Phys. Rev.* **B71** (2005), 045403.
- [Wong et al. 1997] E. W. Wong, P. E. Sheehan, and C. M. Lieber, “Nanobeam mechanics: elasticity, strength, and toughness of nanorods and nanotubes”, *Science* **277**:5334 (1997), 1971–1975.
- [Yakobson and Smalley 1997] B. I. Yakobson and R. Smalley, “Fullerene nanotubes: $C_{1,000,000}$ and beyond”, *Am. Sci.* **85** (1997), 324–337.
- [Yakobson et al. 1996] B. I. Yakobson, C. J. Brabec, and J. Bernholc, “Nanomechanics of carbon tubes: instabilities beyond linear response”, *Phys. Rev. Lett.* **76**:14 (1996), 2511–2514.
- [Yakobson et al. 1997] B. I. Yakobson, M. P. Campbell, C. J. Brabec, and J. Bernholc, “High strain rate fracture and C-chain unraveling in carbon nanotubes”, *Comput. Mater. Sci.* **8**:4 (1997), 341–348.
- [Zhang et al. 2002] P. Zhang, Y. Huang, P. H. Geubelle, P. A. Klein, and K. C. Hwang, “The elastic modulus of single-wall carbon nanotubes: a continuum analysis incorporating interatomic potentials”, *Int. J. Solids Struct.* **39**:13–14 (2002), 3893–3906.
- [Zhang et al. 2004] Y. Q. Zhang, G. R. Liu, and J. S. Wang, “Small scale effects on buckling of multiwalled carbon nanotubes under axial compression”, *Phys. Rev.* **B70** (2004), 205430.

Received 2 Dec 2005.

QUAN WANG: qzwang@mail.ucf.edu

*Department of Mechanical and Manufacturing Engineering, University of Manitoba,
Winnipeg, Manitoba R3T 5V6, Canada*

YASUhide SHINDO: shindo@msws.material.tohoku.ac.jp

*Department of Materials Processing, Graduate School of Engineering, Tohoku University,
Sendai 980-8579, Japan*